The Search for Neutrino Oscillations $\bar{\nu}_\mu \rightarrow \bar{\nu}_e$ with KARMEN

T.E. JANNAKOS for the KARMEN Collaboration
Forschungszentrum Karlsruhe, Institut für Kernphysik I,
D-76021 Karlsruhe, Postfach 3640, Germany
e-mail: thomas.jannakos@bk.fzk.de

KARMEN, the **KA**rlsruhe **R**utherford **M**edium Energy **N**eutrino experiment, is located at the pulsed spallation neutron source ISIS of the Rutherford Appleton Laboratory. In the ISIS beam stop ν_μ, ν_e and $\bar{\nu}_\mu$ are produced from the π^+-μ^+ decay chain at rest with energies up to 52.8 MeV. Besides a very low $\bar{\nu}_e$ contamination, ISIS stands out for its unique time structure. This allows for a highly sensitive search for $\bar{\nu}_\mu \rightarrow \bar{\nu}_e$-oscillations with the KARMEN detector, a 56 t segmented liquid scintillation calorimeter with very good time, energy and position resolution. In 1996 an additional third veto counter was installed within the 7000 t steel blockhouse that shields the detector against cosmic induced background. Covering the detector from all sides it strongly reduces the background of cosmic induced high energy neutrons by a factor of 40. Here we present the data taken after this major upgrade from Feb. 1997 until Feb. 1999. Since there is no indication for any beam excess, an upper limit for the $\bar{\nu}_\mu \rightarrow \bar{\nu}_e$ oscillation is deduced using the Unified Approach based on a maximum likelihood analysis. The result, as all the data presented before, does not support the interpretation of the LSND beam excess as an indication for $\bar{\nu}_\mu \rightarrow \bar{\nu}_e$ oscillation.

1 Introduction

The search for neutrino oscillations is one of the most fascinating topics of modern particle physics. The **KA**rlsruhe **R**utherford **M**edium **E**nergy **N**eutrino experiment KARMEN searches for neutrino oscillations in different appearance ($\nu_\mu \rightarrow \nu_e$ [1] and $\bar{\nu}_\mu \rightarrow \bar{\nu}_e$) and disappearance modes ($\nu_e \rightarrow \nu_x$[2]). The physics program of KARMEN also includes the investigation of ν–nucleus interactions [3] as well as the search for lepton number violating decays of pions and muons and a test of the V–A structure of the μ^+ decay [4]. In the following we present the result of the search for $\bar{\nu}_\mu \rightarrow \bar{\nu}_e$ oscillation on the basis of the data taken from February 1997 until February 1999 (KARMEN 2 data) after the experiment upgrade in 1996. The data taken before the upgrade from 1990 - 1995 (KARMEN 1 data) is not included in the analysis. Such a combined analysis would yield a much lower sensitivity due to the relatively high cosmic induced neutron background of the KARMEN 1 data. In the data set presented here we measure the expected number of background events. Therefore we used the Unified Approach [6] based on a maximum likelihood analysis to derive a 90 % confidence interval.

2 Neutrino Production and Detection

The KARMEN experiment utilizes the neutrinos produced by the neutron spallation source ISIS of the Rutherford Appleton Laboratory in Chilton, Oxon, UK. An intense beam (200 μA) of protons is accelerated to an energy of 800 MeV by a rapid cycling synchrotron. The two parabolic proton pulses of 100 ns base width and a gap of 225 ns are produced with a repetition frequency of 50 Hz (duty cycle is 10^{-5}). The protons are stopped in the compact tantalum beam stop. Apart from spallation neutrons a large number of pions is produced and stopped immediatly within the target. While almost all π^- undergo nuclear capture, the π^+ decay at rest (DAR) into μ^+ and ν_μ. The μ^+ are also stopped within the target and decay at rest via $\mu^+ \rightarrow e^+ + \nu_e + \bar{\nu}_\mu$. The minor fraction of π^- that decays in flight (0.65 % relative to π^+ DAR) with an again suppressed subsequent μ^- decay leads to an extreme small $\bar{\nu}_e$ contamination of $\bar{\nu}_e/\nu_e \leq 6.2 \cdot 10^{-4}$ [7]. The energy spectra of the neutrinos are well defined due to the DAR of both the π^+ and μ^+. The ν_μ from π^+-decay is monoenergetic with E(ν_μ)=29.8 MeV; the continuous energy distributions up to 52.8 MeV of the ν_e and $\bar{\nu}_\mu$ can be calculated using the V-A theory and show the typical Michel shape. Therefore ISIS is a unique, isotropic source of ν_μ, ν_e and $\bar{\nu}_\mu$ from π^+-μ^+ DAR that stands out for its time structure, the small $\bar{\nu}_e$ contamination and the well defined time and energy distribution of the produced neutrinos.

These neutrinos are detected with the KARMEN detector, a segmented calorimeter of 56 t of liquid scintillator. The matrix structure consists of 512 ($32\ rows \times 16\ columns$) optically independent modules with a cross section of 17.4 $\times$ 17.8 cm^2 and a length of 353 cm. The segmentation is made of thin double acrylic walls separated by a small air gap. Every module is read out by two 3 inch photo tubes at each end. The position of an event within one module is given by the time difference between the photo tubes at both ends. The optimized optical properties of the organic liquid scintillator and an active volume of 96% result in an energy resolution of $\sigma_E = 11.5\%/\sqrt{E[MeV]}$. Gd_2O_3 coated paper within the module walls provides an efficient detection of thermal neutrons owing to the very high capture cross section of the Gd (n, γ) reaction ($\sigma \approx 49000$ barn). The KARMEN electronics is synchronized to the ISIS proton pulses to an accuracy of $\pm$2 ns to fully exploit time structure of the neutrinos. The detector is well protected against beam correlated background as well as the hadronic component of the cosmic radiation by a blockhouse made of 7000 t of steel. Cosmic muons entering or stopping close to the detector are identified by the two inner veto counters. The innermost veto covers the calorimeter from four sides and consists of modules identical to those of the

calorimeter but half their width. The second veto counter is made of 136 plastic scintillator modules that shield the detector from five sides. With this configuration (KARMEN 1), the dominant background for the search for $\bar{\nu}_\mu \rightarrow \bar{\nu}_e$ oscillations were high energetic neutrons produced by cosmic muons within the steel blockhouse. To eliminate this background source an additional third veto counter made of 136 plastic szintillator modules with a total area of $300\,m^2$ was installed in 1996 [8]. It was placed right inside the steel blockhouse such that every muon is detected that could produce a neutron within the blockhouse at a distance of up to 1 m from the detector. With this configuration (KARMEN 2) cosmic induced background is considerably reduced by a factor of 40.

3 $\bar{\nu}_\mu \rightarrow \bar{\nu}_e$ oscillation signature

The probability for $\bar{\nu}_\mu \rightarrow \bar{\nu}_e$ oscillations can be written in a simplified 2 flavor description as

$$P(\bar{\nu}_\mu \rightarrow \bar{\nu}_e) = \sin^2(2\,\Theta) \cdot \sin^2(1.27 \frac{\Delta m^2 L}{E_\nu}) \qquad (1)$$

where L is given in meters, E_ν is the neutrino energy in MeV, and Δm^2 denotes the difference of the squared mass eigenvalues $\Delta m^2 = |m_1^2 - m_2^2|$ in eV^2/c^4. The signature for the detection of a $\bar{\nu}_e$ is a spatially correlated, delayed coincidence of a positron from $p(\bar{\nu}_e, e^+)n$ with energies up to $E_{e^+} = E_{\bar{\nu}_e} - Q = 52.8 - 1.8 = 51.0\,MeV$ followed by the γ emission of either of the two neutron capture processes $p(n,\gamma)$ or $Gd(n,\gamma)$. The $p(n,\gamma)$ reaction leads to one γ with an energy of $E(\gamma) = 2.2\,MeV$ whereas the $Gd(n,\gamma)$ process leads to 3 γ in average with a sum energy of 8 MeV. The positrons are expected with a $2.2\,\mu s$ exponential decrease of to the μ^+ decay after beam on target. The time difference between the e^+ and the capture γ is given by the thermalization, diffusion and capture of the neutron. To suppress cosmic induced background, a positron candidate is accepted only if there is no activity in the central detector and in both inner veto counters up to $24\,\mu s$ before. When only the outermost third veto counter was hit, a dead time of $14\,\mu s$ is applied. Further cuts select sequences of events correlated in space and time: $0.6\,\mu s \leq t_{e+} \leq 10.6\,\mu s$ relative to beam on target, $16\,MeV \leq E_{e+} \leq 50\,MeV$. The cuts on the delayed event are applied as follows: $5\,\mu s \leq t_\gamma - t_{e+} \leq 300\,\mu s$, $E_\gamma \leq 8\,MeV$ and a spatial coincidence volume of $1.2\,m^3$.

4 Background Sources

One of the main advantages for the search of $\bar{\nu}_\mu \rightarrow \bar{\nu}_e$ oscillations with the KARMEN experiment is that the expected background is not only very small but also known with a high percision because most of it can be independently measured by applying different cuts. There are only four different sources of background:

- ν_e induced sequences caused by the exclusive charged current reaction $^{12}C(\nu_e, e^-)^{12}N_{g.s.}$ where the subsequent β decay of the $^{12}N_{g.s.}$ ($\tau = 15.9\,ms$) occurs within the first $300\,\mu s$.
- Neutrino reactions that have a random coincidence with a low energy event from the natural radioactivity inside the detector.
- The small intrinsic $\bar{\nu}_e$ contamination from the π^--μ^- decay chain in the ISIS target.
- Undetected cosmic muons which enter the detector or produce high energy neutrons via deep inelastic scattering in the inner part of the steel blockhouse.

The only background source not accessible to direct measurement is the $\bar{\nu}_e$ contamination. It is calculated using a detailed MC simulation of the ISIS target as well as all pion and muon production and decay or capture reactions [7]. Table 1 lists all background reactions and gives the number of expected events as well as their errors for the above defined cuts.

Table 1: Expected sequences from background reactions within the above specified cuts. Given are the mean values and their errors. Shown in the last row is the number of expected $p(\bar{\nu}_e, e^+)n$ reactions from the $\bar{\nu}_\mu \to \bar{\nu}_e$ oscillation for high Δm^2 ($= 100 eV^2$) assuming maximal mixing (i.e. $\sin^2(2\Theta) = 1$).

Background reaction	events
$^{12}C(\nu_e, e^-)^{12}N_{g.s.}$ reaction	2.6 ± 0.3
ν induced random coincidences	2.3 ± 0.3
$\bar{\nu}_e$ contamination from ISIS	1.1 ± 0.1
cosmic induced background	1.9 ± 0.1
total background	7.8 ± 0.5
$p(\bar{\nu}_e, e^+)n$ reactions for $\sin^2(2\Theta) = 1$	1605 ± 176

5 Maximum Likelihood Analysis

The maximum likelihood (ML) analysis is the most powerful method to infer the strength of a possible signal or to derive an upper limit if such a signal is not seen. Because of some advantages over other methods we use here the Unified Approach [6] recommended by the PDG [9] to derive a 90 % confidence interval from our ML analysis. For our ML analysis every background reaction and a possible oscillation signal are taken into account with their different probability density functions for the time and energy of the prompt event (the e^+) as well as the energy, and the time and position difference relative to the prompt event of the sequential event (the neutron capture). The relative contributions of the individual background sources to the total number of background sequences is fixed whereas the number of oscillation sequences is allowed to vary freely. As an additional information the likelihood function (LF) is weighted with a factor that is the conditional poisson probability of the number of inferred background sequences given the expectation value of the total background. The resulting LF depends on Δm^2 and $\sin^2(2\Theta)$ only, and thus for a given Δm^2 only on the number of oscillation sequences N_O infered (or the number of background sequences N_B , for $N_B = N_{total} - N_O$).

For the Unified Approach we divided the relevant $[\Delta m^2; \sin^2(2\Theta)]$ parameter space in the interval $[(10^{-2} eV^2, 10^2 eV^2); (10^{-4}, 1)]$ using a logarithmically equidistant grid of 90×72 points. At every point on the grid we generate 10000 MC data samples according to the expected background and the given values of Δm^2 and $\sin^2(2\Theta)$ for this point. To these data samples the same ML analysis as to the experimental sample is applied. For every MC sample of this specific point on the grid one calculates the logarithm of the likelihoodratio $\Delta log[L(\Delta m^2; \sin^2 2\Theta)]_{MC}$ of the value of the LF at its global maximum in the $[\Delta m^2; \sin^2(2\Theta)]$ parameter space to the value of the LF at the given point on the grid for which the sample was generated. This procedure gives a characteristic MC generated distribution of $\Delta log[L(\Delta m^2; \sin^2 2\Theta)]_{MC}$ for every point on the grid which is then compared to the $\Delta log[L(\Delta m^2; \sin^2 2\Theta)]_{EXP}$ value of the experimental data set (i.e. the logarithm of the ratio of the experimental LF at its global maximum to its value at a given point on the grid). The 90 % confidence interval (C.I.) is the set of points on the grid for which 90 % of all MC generated $\Delta log[L(\Delta m^2; \sin^2 2\Theta)]_{MC}$ are smaller than the experimental value $\Delta log[L(\Delta m^2; \sin^2 2\Theta)]_{EXP}$. The upper 90 % confidence limit (C.L.) as shown in Fig. 1 is the right border of the 90 % C.I.. The interpretation of this C.L. is that for all parameter combinations Δm^2 and $\sin^2(2\Theta)$ on this curve 90 % of a large number of hypothetical KARMEN experiments would have seen a larger "signal" (i.e. $\Delta log[L(\Delta m^2; \sin^2 2\Theta)]_{EXP}$) than the one actually observed.

6 Result and Conclusion

The results presented here are based on the data recorded in the measuring period from February 1997 to February 1999 which corresponds to 4670 C protons on target compared to 2897 C (Feb. 97-Apr. 98) for the data previously presented on conferences [5] where no sequence was observed. Since we now find 5 sequences (4.8 ± 0.3 expected background) within the cuts specified in [5] we relaxed those cuts in order to perform a ML analysis. Within these new cuts as defined in sect. 3 we now observe 8 sequences which has to be compared to the expectation value of the background of 7.8 ± 0.5 sequences. Owing to the fact that none of the prompt events has an energy above 36 MeV the LF has its global maximum in the unphysical region of negative $\sin^2(2\Theta)$ which for a null result is as probable as a slightly positive value. For large Δm^2 ($=100\,eV^2$) the 90 % C.L. is at $\sin^2(2\Theta)=2.1 \cdot 10^{-3}$ and close to the sensitivity [a] at $\sin^2(2\Theta)=2.3 \cdot 10^{-3}$. Why the limit is slightly "better" than the sensitivity (see Fig. 1), is easily explained by the fact that although we observe slightly more sequences than expected, none of these has a prompt event with energies above 36 MeV where – depending on Δm^2 – roughly half of all oscillation sequences should be (and only 1.0 ± 0.1 background sequences are expected). The 90 % C.L. that is compared in Fig. 1 to the LSND result [10] excludes most of the LSND favoured region and is thus a strong hint that the LSND beam excess is not due to $\bar{\nu}_\mu \rightarrow \bar{\nu}_e$ oscillations. Furthermore one has to keep in mind that the limit presented in [5] (also shown in Fig. 1) where no sequences were observed is still valid and puts an even stronger constraint on the LSND favoured region. For this data set (Feb.97 - Apr.98) we expected 2.8 ± 0.1 background sequences. This yields, using again the unified approach, a 90 % C.L. of $1.3 \cdot 10^{-3}$ for large Δm^2 and a sensitivity of $5.4 \cdot 10^{-3}$, respectively. [b]
KARMEN is still an ongoing experiment and will take data until spring 2001. With an expected total charge of 9200 C the sensitivity of the experiment will then be improved by 40 % to $\sin^2(2\Theta)=1.4 \cdot 10^{-3}$ for large Δm^2.

References

1. B. Zeitnitz *et al.*, Prog. Part. Nucl. Physics **40**, 169 (1998).
2. B. Armbruster *et al.*, Phys. Rev. C **57**, 3414 (1998).
3. R. Maschuw *et al.*, Prog. Part. Nucl. Physics **40**, 183 (1998).
4. B. Armbruster *et al.*, Phys. Rev. Lett. **81**, 520 (1998).
5. B. Zeitnitz *et al.*, to be publ. in Nucle. Phys. **B** Proceedings. hep-ex/98 09 007
6. G.J. Feldman and R.D. Cousins, Phys. Rev. D **57**, 3873 (1998).
7. R.L. Burman et al., Nucl. Instr. Meth. A **368**, 416 (1996).
8. G. Drexlin *et al.*, Prog. Part. Nucl. Physics **40**, 193 (1998).
9. R.M. Barnett et al. (Particle Data Group), Phys. Rev. **D 54** 1 (1996).
10. C. Athanassopoulos *et al.*, Phys. Rev. C **54**, 2685 (1996). G.B. Mills, these proceedings
11. M. Appolonio *et al.*, Phys. Lett. B **420**, 397 (1998). D. Nicolo, these proceedings
12. B. Achkar *et al.*, Nucl. Phys. B **434**, 503 (1995).

[a] Since the actual limit of an experiment is affected by statistical fluctuations the sensitivity is defined as the mean confidence limit of a large number of hypothetical but otherwise identical experiments [6].

[b] If one accepts the Unified Approach one must NOT argue that this ("lucky") limit is not trustworthy because it is too far off the sensitivity. This would mean to reduce the Unified Approach and its frequentists ansatz to absurdity.

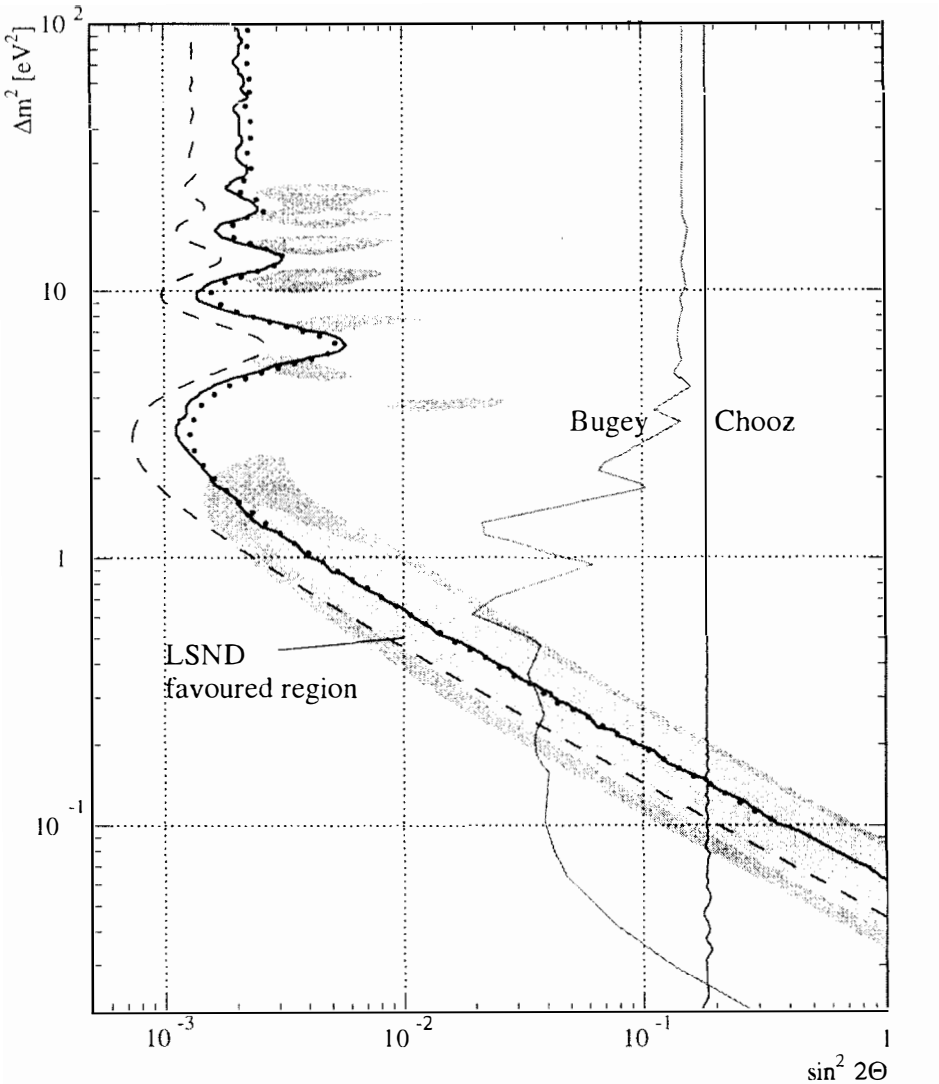

Figure 1: KARMEN 2 90 % confidence limits and sensitivity according to the Unified Approach compared to other experiments: The full line is the 90 % C.L. of the data presented here, the dotted line the corresponding sensitivity and the dashed line the 90 % C.L. derived from the Feb. 97-Apr. 98 data. Also shown are the 90 % C.L. of the two reactor experiments Chooz [11] and Bugey [12] and the favoured region for $\bar{\nu}_\mu \rightarrow \bar{\nu}_e$ oscillations as reported by LSND [10].